

Comparison of multi-mode dynamics in single section Quantum Well and Quantum Dot lasers

Javad Rahimi, Paolo Bardella, Lorenzo Luigi Columbo, Mariangela Gioannini
 Dipartimento di Elettronica e Telecomunicazioni, Politecnico di Torino, Torino, Italy
 *mariangela.gioannini@polito.it

Abstract—We numerically study the effect of carrier grating originated by standing wave pattern on the multi-mode dynamics of semiconductor lasers toward the generation of optical frequency combs. The numerical analysis shows that, due to the localization of the carriers in the quantum dot (QD) active region, the carrier grating guarantees the simultaneous lasing of several optical lines with low mode partition noise, whereas this behavior is not observed in quantum well (QW) lasers because of the carrier diffusion in the active layer.

Keywords—Fabry–Perot laser, Quantum Dot, Quantum Well, Comb lasers, Multi-Mode laser dynamics.

INTRODUCTION

Multi-mode dynamics in single section Fabry–Perot (FP) lasers has been studied since long time. Recently, it turned of practical interest after the experimental demonstration of optical frequency combs in single section quantum well [1], quantum dot or dash [2] and quantum cascade [3] lasers. The numerical study of multi-mode dynamics relies on time-domain travelling wave approaches [4-7] including coherent interaction of the optical electric field with the semiconductor medium [5, 6]. These accurate numerical tools predict quite well the laser dynamics in the multi-wavelength lasers [4, 8], but, due to their complexity, it is often difficult to discriminate the various physical effects at the origin of the dynamics. A multi-mode rate equation approach [9] can be a simple and viable solution for a general understanding of the most important physical effect and it has been applied in [9] to study QW lasers. Our aim is extending the model to the QD lasers case and to compare QW and QD lasers dynamics. We demonstrate that QD lasers have unique properties that, respect to the QW case, allow for stable optical comb generation (i.e.: equally spaced optical lines with stable and equal intensity in time).

NUMERICAL MODEL

Following the approach in [9], we consider a closed cavity FP laser with a cavity length L , supporting only one single transverse mode. To study the temporal evolution of the complex mode field amplitudes as well as the carrier dynamics, a set of ordinary differential equations is considered. The electric field is expanded as $E(z,t) = \sum_j E_j(t) \psi_j(z) \exp(i\omega_j t)$, where $\{\psi_j(z)\}$ is a complete and orthonormal set of base functions for the cavity modes [9]; $E_j(t)$ is the amplitude of the complex mode

and ω_j is the angular pulsation of the j th-mode of the cold cavity. For the QW case we consider only one rate equation for the carriers $N(z,t)$ and we include the diffusion term [9] accounting for spatial diffusion of the carriers in the QW layer. In the QD case we consider two carrier rate equations: one for the WL reservoir, $N_{WL}(z,t)$, and one for the ground state carriers, $N_{GS}(z,t)$. We neglect diffusion because carriers are localized in the zero-dimensional ground state. By considering a set of real base functions as $\varphi_0(z) = 1/\sqrt{L}$ and $\varphi_n(z) = \sqrt{2/L} \cos(n\pi z/L)$, we can expand the variation of the carrier densities respect to the threshold values as excess-inversion moments: $N_n(t) = \sqrt{L} \int_0^L dz [N(z,t) - N_{thr}] \varphi_n(z)$ and $N_{(GS,WL)n}(t) = \sqrt{L} \int_0^L dz [N_{GS,WL}(z,t) - N_{(GS,WL)thr}] \varphi_n(z)$ for the QW and QD lasers, respectively [9].

With these assumptions, we obtain sets of rate equations describing the temporal evolution of the inversion moments and of the complex field of the modes in the cavity. For the QW case, this set corresponds to [9]:

$$\frac{d}{dt} E_k = \frac{g_k - \Gamma_k}{2} E_k + \sum_{j:n} \frac{f_{kj;n} \xi_j}{2} (1 + i\alpha_j) N_n E_j e^{i\omega_{jk} t} \quad (1)$$

$$\begin{aligned} \frac{d}{dt} N_n = \Delta J_n - \frac{N_n}{T_n} - \text{Re} \sum_{jk} g_j f_{jk;n} E_j^* E_k e^{i\omega_{kj} t} \\ - \text{Re} \sum_{jkm} \xi_j (1 + i\alpha_j) f_{jk;nm} N_m E_j^* E_k e^{i\omega_{kj} t} \end{aligned} \quad (2)$$

where the coupling coefficients are calculated as: $f_{kj;n} = \sqrt{L} \int_0^L dz \psi_k^*(z) \psi_j(z) \varphi_n(z)$ and $f_{jk;nm} = L \int_0^L dz \psi_j^*(z) \psi_k(z) \varphi_n(z) \varphi_m(z)$. ΔJ_n is the n -th moment of the excess injection current; the other coefficients are defined in Table I.

The QD rate equations set, not reported in [9] and original result of this study, is presented in the following equations; the coefficients are defined in Table I. Respect to the QW case, we have not only the f coupling coefficients, but also the additional $r_{mm'n}$ coupling terms that originate from the carrier coupling between GS and WL via capture and escape processes.

$$\frac{d}{dt} E_k = \frac{g_k - \Gamma_k}{2} E_k + \sum_{j:n} \left(\frac{i\gamma}{L} N_{WL_n} + \frac{1 + i\alpha_j}{\tau_{g_j}} \frac{N_{GS_n}}{\mu} \right) E_j f_{kj;n} e^{i\omega_{jk} t}$$

$$\begin{aligned} \frac{d}{dt} N_{WL_n} = \Delta J_n + \frac{L}{\mu \tau_c} (N_{GS_{th}} N_{WL_n} + N_{WL_{th}} N_{GS_n}) \\ + \sum_{mm'} r_{mm'n} \frac{N_{WL_m}}{\tau_c} \frac{N_{GS_{m'}}}{\mu} - \frac{N_{WL_n}}{\tau_{nr,WL}} - \frac{N_{WL_n}}{\tau_c} + \frac{N_{GS_n}}{\tau_{esc}} \end{aligned}$$

This work is supported by Fondazione CRT under the initiative “La Ricerca dei Talenti”.

Table I. Physical parameters and corresponding values

Cavity length $L=1$ mm	QD threshold gain $g_{th}=0.1$ ps ⁻¹
Modes num $k,j=1000,1001,1002$	QD Henry coefficient $\alpha=0$
QW losses $\Gamma_k=1$ ps ⁻¹	QD gain time constant $\tau_{g_i}=6$ ps
QW threshold gain $g_k=1$ ps ⁻¹	GS capture, escape time $\tau_c=1$ ps, $\tau_{esc}=2.3$ ps
QW Henry coefficient $\alpha=3$	GS degeneracy $\mu=2$
QW differential gain $\xi_i=5$ ms ⁻¹	Non radiat. lifetime $\tau_{nr,WL}=900$ ps, $\tau_{nr}=2$ ns
QD losses $\Gamma_k=0.1$ ps ⁻¹	Plasma refractive index change $\gamma=52.1$ m ³ /s

$$\frac{d}{dt} N_{GS_n} = \frac{N_{WL_n}}{\tau_c} - \frac{N_{GS_n}}{\tau_{esc}} - \frac{N_{GS_n}}{\tau_{nr}} - \frac{N_{GS_{th}}}{\mu} \frac{LN_{WL_n}}{\tau_c} + \frac{N_{GS_n}}{\mu} \frac{LN_{WL_{th}}}{\tau_c}$$

$$- \sum_{mm'} \frac{r_{mm'n} N_{WL_m}}{\tau_c} \frac{N_{GS_{m'}}}{\mu} - 2 \operatorname{Re} \sum_{jkm} f_{jk;nm} \frac{1+i\alpha_j}{\tau_{g_j}} \frac{N_{GS_m}}{\mu} E_k E_j^* e^{i\omega_{kj}t}$$

$$- \frac{2\gamma}{L} \operatorname{Re} \sum_{jkm} i f_{jk;nm} N_{WL_m} E_k E_j^* e^{i\omega_{kj}t} - \operatorname{Re} \sum_{jk} f_{kj;n} g_j E_k E_j^* e^{i\omega_{kj}t}$$

SIMULATION RESULTS AND DISCUSSION

To focus the comparison between the QW and QD laser dynamics, we consider as simple test case a 3-mode laser with mode spacing of 40 GHz and we numerically solve the rate-equation systems. In the QW case, the carrier inversion moments are only those slow ones related to the neighboring mode beating (i.e. N_0 , N_1 , and N_2), because carrier diffusion washes out the faster spatial variations. In the QD case, the diffusion is not present and we include the fast inversion moments N_{2k} and N_{2k+1} . These terms are the carrier gratings originated by the standing wave pattern in the FP cavity due to each k -th mode (N_{2k}) and due the beating between forward and backward propagating adjacent modes k and $k+1$.

To study and compare the multi-mode behavior, we calculate first the optical spectrum of the total field, then we filter out each optical frequency line and we evaluate the temporal dynamics of the line intensities. Fig. 1 summarizes the typical QW dynamics: the three optical lines (evidenced by the three colors in Fig. 1a) exhibit strong mode partition noise (Fig. 1b) with the central line very attenuated respect to the other two. The intensity fluctuations increase with current (Fig. 1c).

A completely different dynamics is observed in the QD case of Fig. 2. The three optical lines (Fig. 2a) are narrower than in the QW case, the mode partition noise is negligible (Fig. 2b) and the power of the three lines keeps almost equal increasing

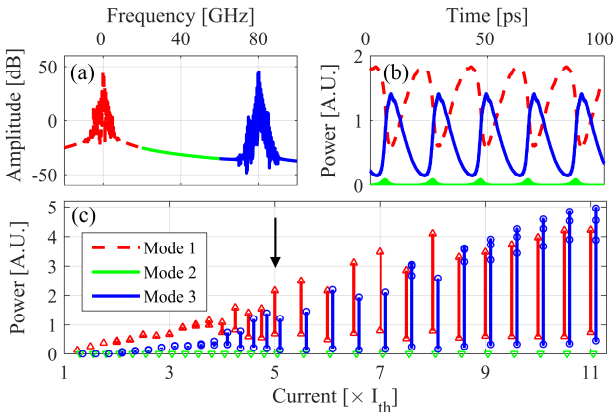


Fig. 1. QW laser case: (a) optical spectrum of the total electric field (centered at the reference frequency) and (b) power versus time of each optical line at $5I_{th}$. (c) Bifurcation diagram of the output power of each line. The arrow indicates the case addressed in (a) and (b).

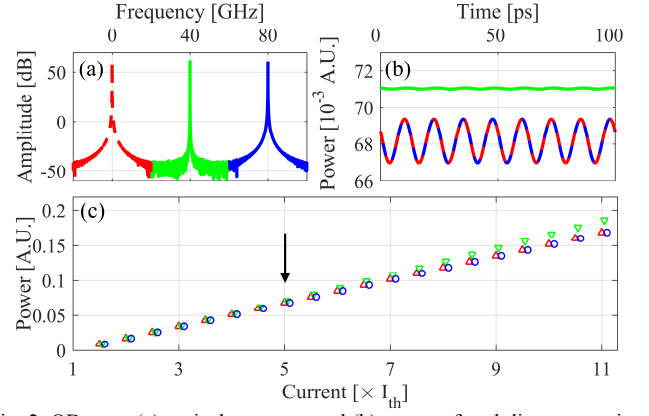


Fig. 2. QD case: (a) optical spectrum and (b) power of each line versus time at $5I_{th}$. (c) Bifurcation diagram of the output power of each line.

current (Fig. 2c). This behavior is peculiar of the QD laser and can be reproduced only if the fast N_{2k} inversion moments are included in the model. If these fast carrier gratings are forced to zero, we get unstable states with mode hopping.

To verify the possibility of generating an optical comb even in presence of waveguide and material dispersion, we consider in Fig. 3 a QD laser with three unequally spaced cold cavity modes centered at 0 GHz, 40.1 GHz and 79.9 GHz. For currents smaller than 15 times threshold current, the dynamics is dominated by strong partition noise and broad optical lines. At $15I_{th}$ we observe an abrupt switch to an optical comb regime with no partition noise and almost same power on the lines. When the light intensity becomes high enough to guarantee a sufficiently strong FWM, the mode coupling allows the phase pooling and locking of the lines. The current value at which this transition occurs depends on the asymmetry in the cold cavity mode spacing and can be reduced decreasing this asymmetry.

REFERENCES

- [1] C. Calò et al., Optics Express 23, 20 (2015).
- [2] K. Merghem et al., IEEE J. Quantum Electron 50, 4 (2014).
- [3] J. Faist et al., Nanophotonics, 5, 2 (2017)
- [4] J. Javaloyes and al., "Freetwm" (2012) <http://onl.uib.eu/software>
- [5] C.Z. Ning, IEEE J. Quantum Electron 33, 9 (1997).
- [6] P. Bardella et al., CLEO Europe (2017).
- [7] A. Gordon et al., Phys. Rev. A. 77, 053804 (2008).
- [8] M. Giovannini et al., IEEE J. Quantum Electron 21, 1900811 (2015).
- [9] M. Yousefi et al., Proc. SPIE 8980 (2014).

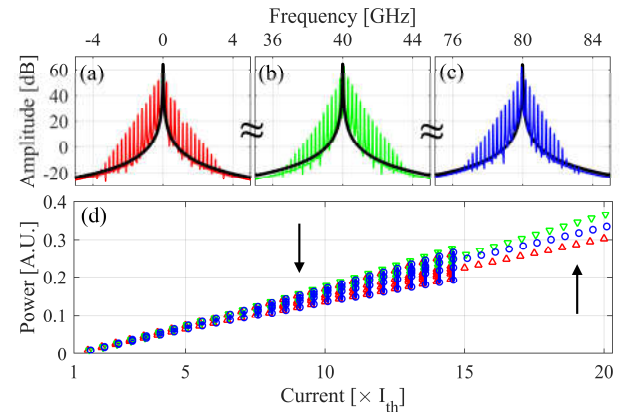


Fig. 3. QD case showing the cold cavity modes at (a) 0, (b) 40.1GHz and (c) 79.9 GHz; black narrow lines are $18I_{th}$ when locking is achieved; coloured lines are at $8I_{th}$. (d) Bifurcation diagram of the power of each line.